ACS Medicinal Chemistry Letters

pubs.acs.org/acsmedchemlett Letter

Design and Implementation of Synthetic RNA Binders for the Inhibition of miR-21 Biogenesis

Chloé Maucort, Duc Duy Vo, Samy Aouad, Coralie Charrat, Stéphane Azoulay, Audrey Di Giorgio, and Maria Duca*

Cite This: ACS Med. Chem. Lett. 2021, 12, 899−906

Read Online

ACCESS | Metrics & More | Article Recommendations | Supporting Information

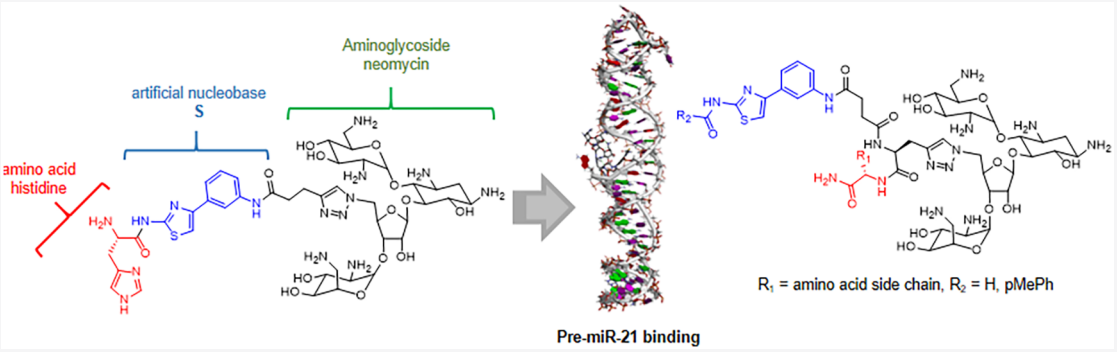

ABSTRACT: Targeting RNAs using small molecules is an emerging field of medicinal chemistry and holds promise for the discovery of efficient tools for chemical biology. MicroRNAs are particularly interesting targets since they are involved in a number of pathologies such as cancers. Indeed, overexpressed microRNAs in cancer are oncogenic and various series of inhibitors of microRNAs biogenesis have been developed in recent years. Here, we describe the structure-based design of new efficient inhibitors of microRNA-21. Starting from a previously identified hit, we performed biochemical studies and molecular docking to design a new series of optimized conjugates of neomycin aminoglycoside with artificial nucleobases and amino acids. Investigation about the mode of action and the site of the interaction of the newly synthesized compounds allowed for the description of structure−activity relationships and the identification of the most important parameters for miR-21 inhibition.

KEYWORDS: *RNA ligand, microRNA, cancer, inhibitor, RNA targeting*

Targeting the biogenesis of oncogenic microRNAs using synthetic small molecules has recently been raised as a promising strategy to affect cancer cell growth.[1,2] MicroRNAs (miRNAs or miRs) are short noncoding RNAs that control gene expression upon binding to mRNAs and inhibition of related protein synthesis.[3] Each miRNA is responsible for the expression of hundreds of proteins, and the resulting regulation process is widespread in eukaryotic cells.[4,5] Modifications in miRNA expression have been also recognized as major causes in various pathologies such as cancer.[6] The miRNAs that are overexpressed in cancer are called oncogenic and inhibit the translation of tumor suppressor proteins, while miRNAs that are underexpressed are tumor suppressors and inhibit the translation of oncogenic proteins. Various approaches have thus been developed to tackle these deregulation processes, such as the use of oligonucleotides that replace a lacking tumor suppressor miRNA or directly inhibit the function of an oncogenic one.[7] Small molecules have also been developed as inhibitors of the biogenesis of oncogenic miRNAs, and they have led to great successes in terms of activity and specificity.[1,8,9] More complex compounds, such as nucleobase-peptide libraries, also led to promising results in the context of miRNA inhibition.[10] Among the most important examples, compounds identified using InfoRNA showed high specificity toward the miRNA target, inhibiting its production upon binding to the corresponding pri-miRNA or pre-miRNA.[11,12] Other recently developed methods to predict RNA−ligand interactions, such as RLDOCK, together with target-directed screenings and structure-based probing offer promising perspectives for the identification of RNA binders.[13−16]

Complementary to these works, we recently developed strong pre-miRNAs ligands directed against oncogenic miR-372 biogenesis and able to bind to its precursor pre-miR-

Special Issue: RNA: Opening New Doors in Medicinal Chemistry

Received: December 29, 2020
Accepted: May 3, 2021
Published: May 14, 2021

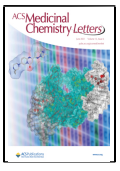

https://doi.org/10.1021/acsmedchemlett.0c00682
ACS Med. Chem. Lett. 2021, 12, 899−906

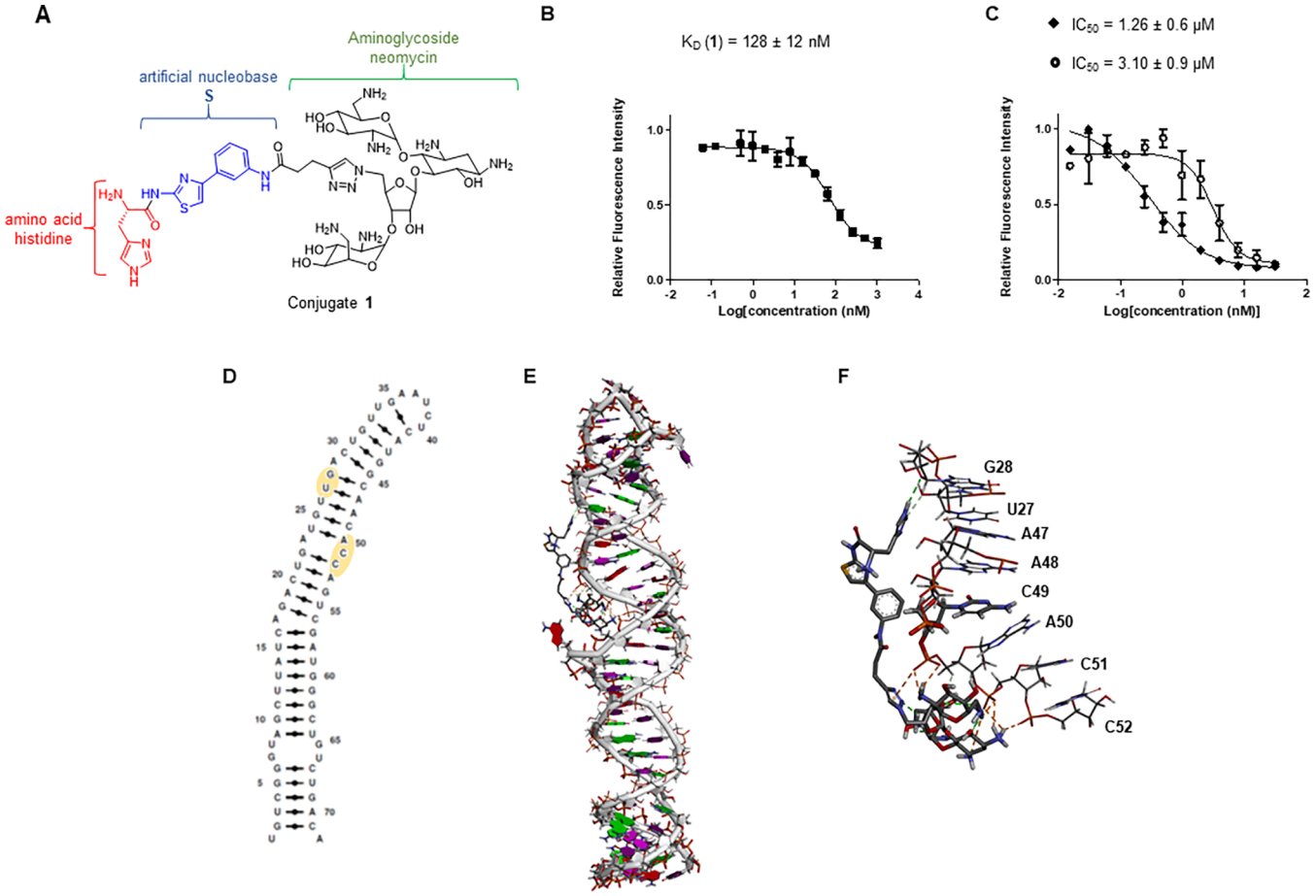

Figure 1. (A) Chemical structure of the conjugate **1**. (B) Dissociation constant (K_D) evaluation for compound **1** and its affinity for the pre-miR-21 sequence. The reported K_D value is expressed in nM and calculated over three independent experiments performed in duplicate. (C) IC_{50} evaluation for compound **1** inhibition of pre-miR-21 processing in the presence of *E. coli* RNase III purified enzyme (◆) and in the presence of MCF-7 lysates (○). Human Recombinant Dicer has also been used and led to very similar values. The reported IC_{50} value is expressed in μM and calculated over three independent experiments performed in duplicate. (D) Structure of pre-miR-21 as reported in the miRbase (www.mirbase.org) with the binding site of **1** highlighted in yellow. (E) Docking of **1** with the pre-miR-21 hairpin loop performed using AutoDock 4, in which the grid boxes were fixed on the entire RNA sequence. (F) Compound **1** and direct interacting residues of pre-miR-21 sequence together with the formed interaction in the complex.

372.[17−19] miR-372 is overexpressed in various cancers, such as gastric cancers, being directly linked to the proliferation of these cancer cells.[20] To identify new inhibitors of this oncogenic miRNA, we designed conjugates between the aminoglycoside neomycin, artificial nucleobases, and amino acids. Aminoglycosides are known RNA ligands employed in the clinic as antimicrobials since they bind to prokaryotic rRNA, thus impairing protein synthesis in bacteria.[21] These antibiotics have known for a long time, but interest in their conjugation for the improvement of biological activity and/or pharmacological profile is still great.[22] Neomycin belongs to this class and represents a strong yet nonspecific RNA ligand.[23] Artificial nucleobases are heterocyclic compounds able to form specific hydrogen bonds with DNA and RNA base pairs.[24] Finally, amino acids, especially basic ones, are also known to bind to RNA as the main constituent of natural RNA ligands, i.e., peptides. The resulting conjugates bear nucleobase **S** reported to interact with an A·U base pair[25] as well as an amino acid (Lys, Arg, or His) and the aminoglycoside neomycin. The strongest inhibitor of this series was conjugate **1** containing histidine amino acid (Figure 1A).[17] Compound **1** showed excellent binding and selectivity for pre-miR-372 in vitro. Also, it inhibited the proliferation of gastric adenocarcinoma (AGS) cells highly overexpressing miR-372, and this inhibition was specific since other cells that do not overexpress miR-372 were not affected. These studies demonstrated that the antiproliferative effect could be linked to the inhibition of miR-372 expression in AGS cells and that this kind of conjugate inhibited in a dose-dependent manner another small set of miRNAs inside cells. Among them, miR-21 was particularly inhibited. miR-21 is a general oncogenic miRNA in various cancers and is responsible for the repression of several important tumor suppressor proteins, thereby representing an interesting anticancer target.[26] Small molecules able to target this oncogenic miRNA have been reported to show the efficacy of this strategy for the development of antiproliferative compounds.[27−31]

To assess how compound **1** affects miR-21 biogenesis, we characterized its binding to pre-miR-21 in vitro. First, the dissociation constant (K_D) was evaluated using previously reported fluorescence-based assays.[18] This kind of assay is based on the fact that binding to RNA induces a conformational change that influences the environment of the probe.[32] The measurement of fluorescence variation upon binding of

https://doi.org/10.1021/acsmedchemlett.0c00682
ACS Med. Chem. Lett. 2021, 12, 899−906

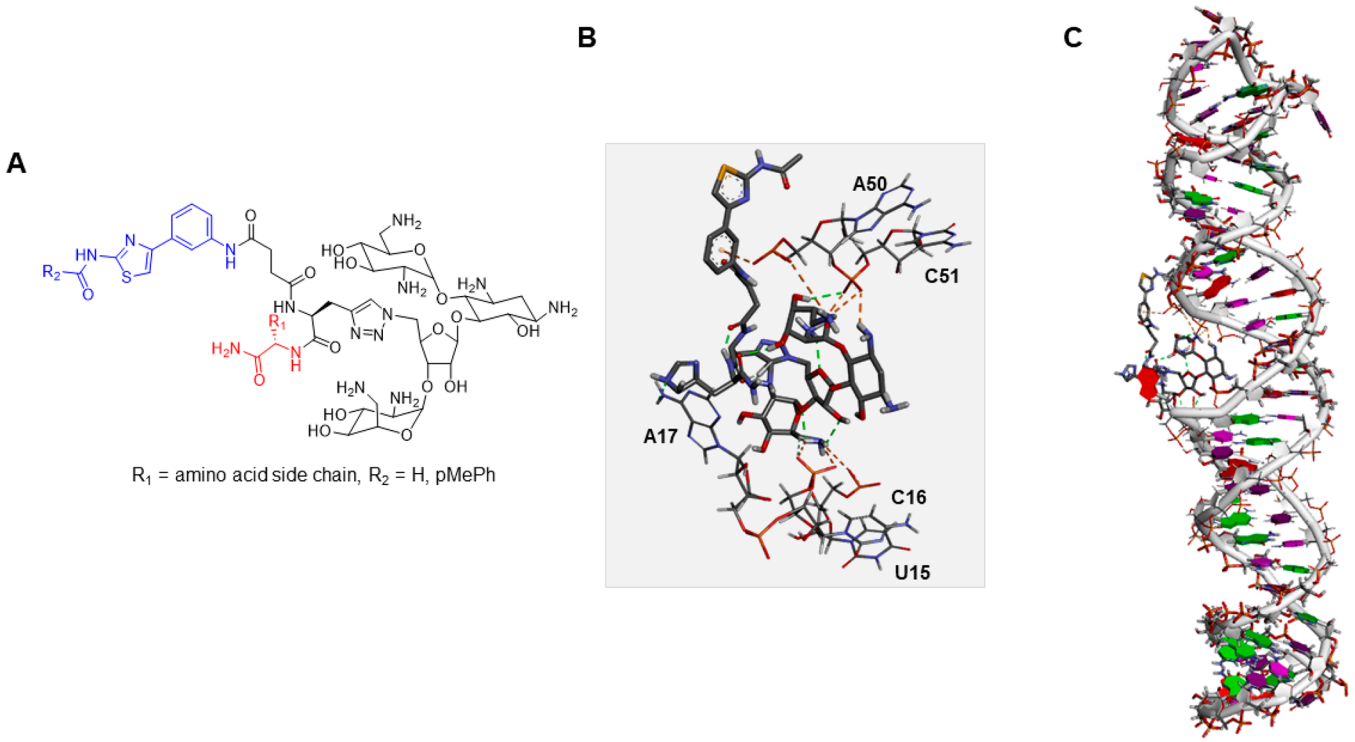

Figure 2. (A) General structure of the new series of conjugates synthesized in this work. (B) Docking of the new conjugate containing neomycin, histidine, and nucleobase S (**6c**) with the pre-miR-21 hairpin loop performed using autodock 4. (C) Compound **6c** and direct interacting residues of pre-miR-21 sequence together with the interactions in the complex.

increasing concentrations of ligands to a 5′-labeled pre-miR-21 thus leads to K_D measurements. As illustrated in Figure 1B, the K_D of compound **1** was 128 ± 12 nM, 10 times lower than the that for neomycin. Selectivity of **1** for pre-miR-21 in the presence of other nucleic acids competitors was then studied, since it is an important parameter for the design of pre-miRNAs inhibitors. We thus measured the K_D in the presence of a large excess (100 equiv) of competitors, such as tRNA and DNA, two intracellular abundant nucleic acid structures. These competition experiments allow for a better understanding of the selectivity against intracellularly highly expressed nucleic acids but also about nonspecific backbone and intercalation interactions of the studied ligands. Compound **1** showed selectivity for pre-miR-21 since K_D values were maintained in the presence of tRNA or DNA (Table 1, entries 1 and 2). Following these preliminary data, the inhibition of Dicer processing of pre-miR-21 was measured using a FRET-based assay where a 5′-fluorescein-3′-dabcyl-labeled pre-miR-21 was employed.[18] Normal cleavage by Dicer enzyme induces an increase in fluorescence, while binding of an appropriate ligand that inhibits cleavage blocks the appearance of fluorescence. Performing this kind of assay over a range of ligand concentrations allows for the measurement of IC_{50} values. The obtained results for compound **1** showed an IC_{50} of 1.26 ± 0.6 μM (Figure 1C and Table S1). This promising result prompted us to evaluate the selectivity of the inhibition activity. We thus measured IC_{50} using the same cell-free assay but in the presence of MCF7 cell lysates instead of recombinant Dicer enzyme, since a large number of protein and nucleic acid competitors are present in the mixture and could impair the activity of **1** on pre-miR-21 if the compound acts nonselectively. Interestingly, promising selectivity of inhibition could be observed when lysates were employed, since the IC_{50} value was 3.10 ± 0.9 μM that represents a 2.5 ratio between the two values. Altogether, these results are promising for the development of compounds of that type against miR-21 production. We thus decided to explore the site of interaction of compound **1** on the pre-miR-21 structure using molecular docking. While Figure 1D shows the primary and secondary structure of pre-miR-21 as reported in the miRbase (www.mirbase.org), Figure 1E and F illustrates the docking of compound **1** performed using AutoDock obtained using the pre-miR-21 hairpin loop after applying the MC-Fold/MC-Sym pipeline to construct a 3D model.[33] The docking studies, that previously showed their valuable results in the study of the interactions between various RNA ligands and pre-miR-21,[19,34] suggested that conjugate **1** interacted with residues U27 to G28 and A50 to C52 that are located close to the cleavage site of the Dicer enzyme (A29/C46) but in the stem part of the pre-miR-21 structure.[35] It has been demonstrated that the stem region of each pre-miRNA (the so-called ruler) is important for the correct positioning of Dicer and that ligands interacting with this region can be efficient inhibitors of pre-miRNAs processing.[36,37] In the context of this possible binding complex, the interaction of **1** with pre-miR-21 could involve the formation of hydrogen bond interactions between the imidazole of histidine and U27 and G28 as well as electrostatic interactions between the neomycin moiety and residues A50 to C52. The triazole seems to also be important as it interacts with residue C49. Finally, it can be noted that the nucleobase does not seem to be involved, illustrating that the spatial distribution of the three binding domains could be suboptimal for efficient binding. We thus decided to explore the possibility to improve the inhibition of miR-21 biogenesis upon chemical modifications that could increase and optimize the interaction network formed. Based

https://doi.org/10.1021/acsmedchemlett.0c00682
ACS Med. Chem. Lett. 2021, 12, 899−906

Scheme 1. Solid-Phase Synthetic Pathway for the Preparation of New Conjugates 6a/a′−6c-c′ Containing Neomycin, Artificial Nucleobase S, and Amino Acids Alanine, Lysine, and Histidine[a]

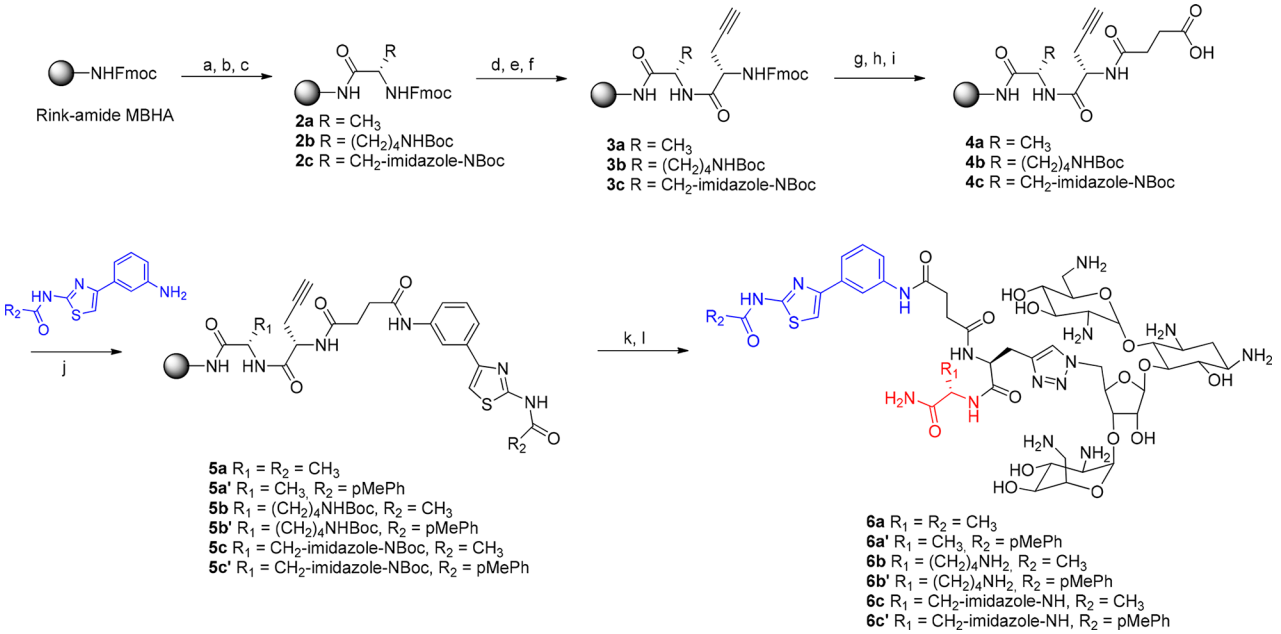

[a]Final compounds were obtained as TFA salts even if the neutral structure was written for clarity. Reagents: (a) piperidine, DMF, rt, 30 min; (b) Fmoc-Ala-OH, Fmoc-Lys-OH, or Fmoc-His-OH, HBTU, DIPEA, DMF, rt, 2 h; (c) Ac_2O, pyr, DMF, rt, 10 min; (d) piperidine, DMF, rt, 30 min; (e) Fmoc-propargyl-Gly, HBTU, DIPEA, DMF, rt, 2 h; (f) Ac_2O, pyr, DMF, rt, 10 min; (g) piperidine, DMF, rt, 30 min; (h) succinic anhydride, DMF, rt, 1 h; (i) Ac_2O, pyr, DMF, rt, 10 min; (j) **S** or **SAr**,[18] iodomethylpyridinium iodide, DIPEA, DMF, rt, 1.5 h; (k) $Neo(Boc)_6N_3$,[17] CuI, DIPEA, DMF, rt, overnight; (l) TFA, TIS, rt, 2 h.

on the intracellular inhibition of miR-21 expression,[17] on the promising values of K_D and IC_{50} obtained during biochemical assays, and on the molecular docking studies described above, we designed compounds bearing a more flexible linker between the neomycin moiety and the nucleobase as well as a different distribution of the RNA binding domains. To this aim, we envisioned modification of the chemical structure of **1** by addition of an aliphatic linker between the triazole and the nucleobase and by placing the amino acid residue on this linker as illustrated in the general structure of Figure 2A. Molecular docking helped us to understand if such compounds could be better pre-miR-21 binders than compound **1**. The docking of a compound of this new series containing histidine as the amino acid (**6c**) is illustrated in Figure 2B and C, and it showed that this compound could indeed interact with pre-miR-21. The docking suggests that the three moieties histidine, **S**, and neomycin could participate to the interaction, opening the possibility for better selectivity and activity compared to **1**. Furthermore, the model suggests that compound **6c** could interact with residues U15 to A17 as well as A50 to C51 via an increased number of hydrogen bonds and electrostatic interactions compared to compound **1**.

Based on these results, we decided to synthesize a new series of compounds bearing the general structure illustrated in Figure 2A. To this aim, we conjugated neomycin to nucleobase **S** that is the one used in the docking study, but also to **SAr**, a similar artificial nucleobase containing a supplementary aryl substituent that was previously shown to be very promising for better interaction with pre-miRNAs.[19] Furthermore, we decided to compare histidine amino acid with alanine to measure the influence of a hydrophobic side chain and with lysine that contain a basic but aliphatic side chain to compare with the histidine imidazole. A control compound containing uracil instead of nucleobase **S** was also prepared to study the influence of the nucleobase on the affinity and biological activity (compound **15**, Scheme S2).

The synthesis of conjugated aminoglycosides for better RNA binding is a challenging field. Many analogues have been reported in the literature, and even if a number of synthetic routes have been explored to conjugate various moieties at different positions on the aminoglycoside, new synthetic approaches are always needed.[38−40] Here, we decided to use a solid-phase synthetic strategy as illustrated in Scheme 1 to avoid purification steps. Rink amide MBHA resin was first deprotected in the presence of piperidine in DMF and the resulting free amine was charged at 50% with the amino acid *Na*-Fmoc-L-alanine (as in **2a**), *Na*-Fmoc-*Nw*-Boc-L-lysine (as in **2b**) or *Na*-Fmoc-N_{Im}-Boc-L-histidine (as in **2c**) in the presence of HBTU, DIPEA in DMF. After capping the unreacted amines with acetic anhydride in the presence of pyridine in DMF, the added amino acid was deprotected by piperidine in DMF and *Na*-Fmoc-L-propargyl-glycine was coupled to the free amine by HBTU in the presence of DIPEA in DMF. Capping by acetic anhydride in pyridine and DMF led to desired intermediates **3a−c**. The Fmoc group was removed again, and the resulting amine was reacted with succinic anhydride in the presence of DIPEA in DMF. Final capping led to desired compounds **4a−c**. This scaffold now contains a free carboxyl group for the introduction of the nucleobase and an alkyne group for the introduction of an azido-substituted neomycin derivative. First, nucleobases **S** and **SAr**[17,19] were coupled to the carboxyl group in the presence of iodomethylpyridinium chloride, DIPEA, and DMF, leading to compounds **5a/a′−5c/c′**. Then, 1,3-dipolar cycloaddition was performed with Boc-protected 5″-azido-neomycin ($Neo(Boc)_6N_3$)[18] in the presence of CuI, DIPEA, and DMF. This

https://doi.org/10.1021/acsmedchemlett.0c00682
ACS Med. Chem. Lett. 2021, 12, 899−906

Table 1. Dissociation Constants (K_D, nM) Measured for Pre-miR-21 Binding Alone or in the Presence of 100 equiv Excess of tRNA (K_D', nM) or 100 equiv Excess of DNA Duplex (K_D'', nM)

entry	ID	K_D [nM][a] pre-miR-21	K_D' [nM] (tRNA competition)	K_D'/K_D	K_D'' [nM] (DNA competition)	K_D''/K_D
1	neomycin	1390 ± 126	1415 ± 110	1.0	1950 ± 20.2	1.4
2	**1**	128 ± 12	134 ± 14	1.0	171 ± 16	1.3
3	**6a**	133 ± 20	151 ± 13	1.1	187 ± 24	1.4
4	**6a′**	128 ± 7.0	170 ± 48	1.3	261 ± 60	2.0
5	**6b**	50.7 ± 7.4	51.0 ± 8.7	1.0	95.7 ± 22	1.9
6	**6b′**	348 ± 34	405 ± 138	1.2	877 ± 79	2.5
7	**6c**	50.3 ± 11	50.4 ± 7.0	1.0	80.9 ± 3.2	1.6
8	**6c′**	162 ± 40	168 ± 10	1.0	274 ± 30	1.7
9	**15**	641 ± 165	807 ± 270	1.3	1459 ± 70	2.3

[a]Binding studies were performed on 5′-FAM-pre-miR-21 in buffer A (20 mm Tris−HCl (pH 7.4), 12 mm NaCl, 2.5 mm $MgCl_2$, and 1 mm DTT).

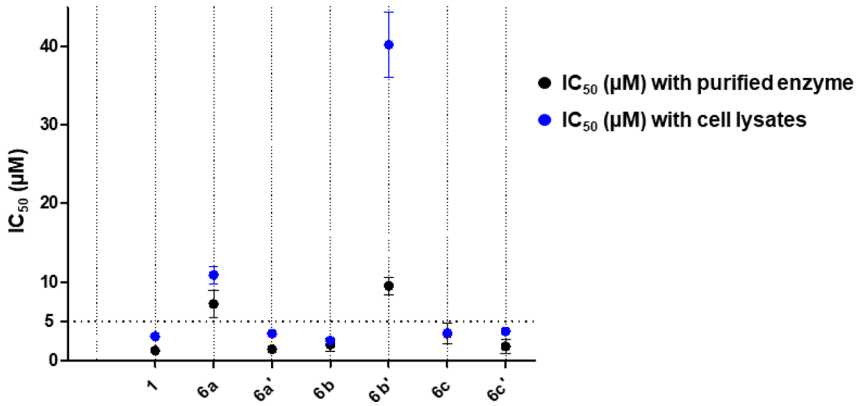

Figure 3. IC_{50} values of compounds **6a**/**a′**−**6c**/**c′** against pre-miR-21 72-mer fragment labeled at the 5′-end with fluorescein and at the 3′-end with dabcyl measured upon processing with recombinant enzyme (black circle). Selectivity of compounds **6a**/**a′**−**6c**/**c′** for pre-miR-21 in the presence of MCF7 cell lysates (blue circle). IC_{50} values were determined from duplicates performed over three independent experiments.

step needed 4 equiv of CuI (2 × 2 equiv) as Cu adsorbs on the solid support. Then, removal of Boc groups by a mixture of TFA/TIS led simultaneously to resin cleavage as well as the release of large quantities of copper with desired conjugates **6a**/**a′**−**6c**/**c′** which had to be removed by successive treatments with Chelex resin to capture Cu, leading to low overall yields < 20%. To circumvent this constraining purification step, we performed the deprotection/cleavage step before the 1,3-dipolar cycloaddition in order to carry out the click reaction in liquid-phase and to avoid copper accumulation on the solid support. This strategy allowed us to obtain compounds **6a**/**a′** and **6b′** with increased global yields (between 35% and 45%). For comparison, the other compounds (**6b** and **6c**/**c′**) were prepared through a complete liquid-phase synthesis (Supporting Information Scheme S1) and led to final compounds with overall yields similar to the solid phase methodology but with the need for more purification steps. The synthesis of the desired conjugates was thus successful even if their preparation remains complex.

Compounds **6a**/**a′**−**6c**/**c′** were designed in order to improve affinity and inhibition activity against pre-miR-21 and its biogenesis as previously described for **1**. We thus decided to first study the binding affinity toward pre-miR-21 and compare the obtained values with nonconjugated neomycin and parent compound **1**. As mentioned before, we also prepared compound **15** (Scheme S2) containing natural nucleobase uracil instead of artificial nucleobase **S**. As illustrated in Table 1 (and in Supporting Information Figure S1), all conjugated compounds (entries 3−8) bear a K_D in the low nanomolar range, thus showing great improvement in the binding affinity compared to unconjugated neomycin. Compounds containing nucleobase **S** (**1** and **6a**−**c**) bear better affinity than the ones containing **SAr** nucleobase (**6a′**−**6c′**), suggesting that the addition of a phenyl ring on the nucleobase probably hinders the interaction with the target. Indeed, compounds **6a′**, **6b′**, and **6c′** show K_D values of 128, 348, and 162 nM, respectively, thus being weaker binders than the corresponding **S** derivatives **6a**, **6b**, and **6c**. While compound **6a** showed a K_D value of 133 nM, compounds **6b** and **6c** showed K_D values of 50.7 and 50.3 nM, respectively, representing a 2.5-fold improvement in comparison with compound **1**. This also illustrates that a positively charged and hydrophilic amino acid side chain is important for interaction since **6b** and **6c** containing lysine and histidine, respectively, have better affinity for the target than **6a** containing alanine. Interestingly, compound **15** containing uracil instead of **S** bears a K_D of 641 nM that is a 13-fold higher value compared to that of **S** conjugates, illustrating that the artificial nucleobase also plays an important role in pre-miR-21 binding. This suggests that the spatial distribution of these new compounds could be more favorable for the involvement of the nucleobase in the interaction compared to what observed for compound **1**. Selectivity studies in the presence of tRNA or DNA showed that the ratios between K_D' (dissociation constant in the presence of tRNA) or K_D'' (dissociation constant in the presence of DNA) and K_D are close to 1 (Table 1, entries 3−9). Only compounds **6a′**, **6b′**, and **15** showed slightly higher values.

Based on these binding data, we wondered whether these compounds could be good inhibitors of its processing. We thus

https://doi.org/10.1021/acsmedchemlett.0c00682
ACS Med. Chem. Lett. 2021, 12, 899−906

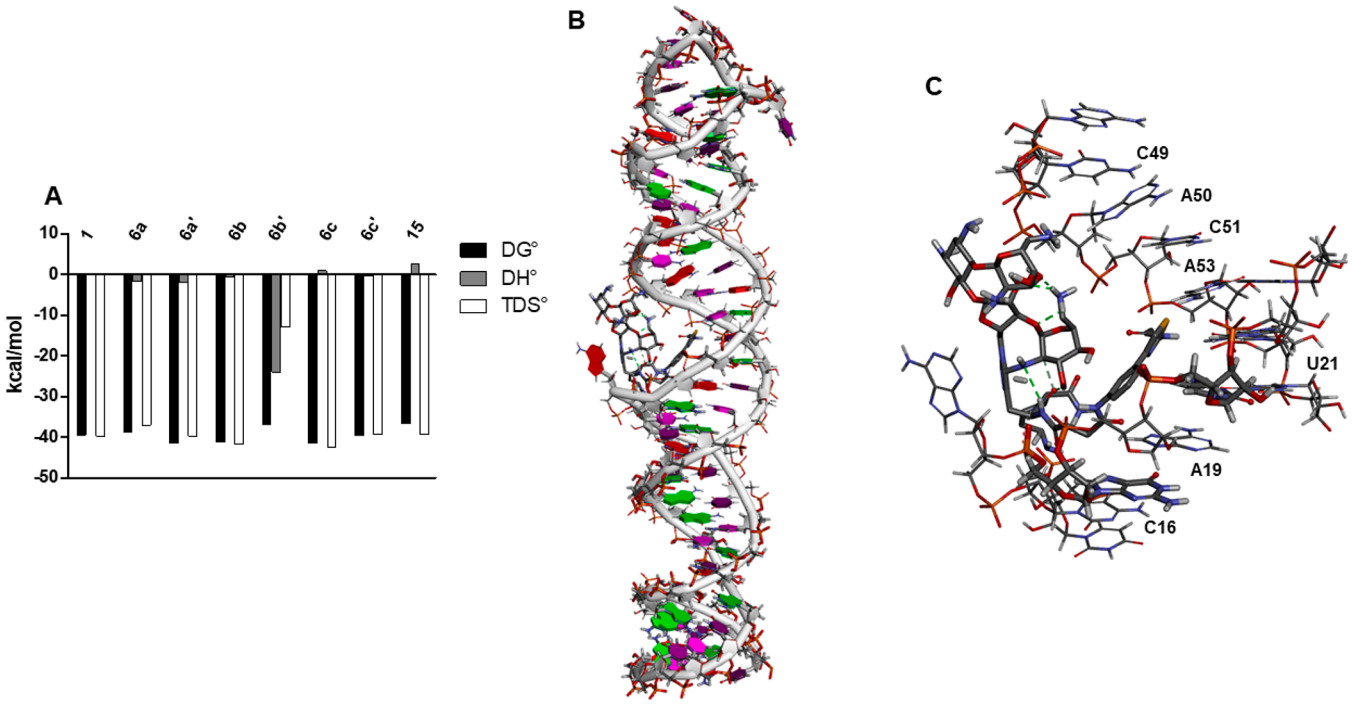

Figure 4. (A) Thermodynamic profiles for the high-affinity binding of heterocycle-spermine conjugates **1** and **6a**/**a**′−**6c**/**c**′ to the pre-miR-21 at 20 °C: $\Delta G°$ (black bars), $\Delta H°$ (dark gray bars), and $-T\Delta S°$ (light gray bars). (B) Molecular docking of **6b** in interaction with pre-miR-21 hairpin loop performed using AutoDock 4 wherein the grid boxes were fixed on the entire RNA sequence. (C) Compound **6b** and direct interacting residues of pre-miR-21 sequence together with the interactions in the complex.

performed the FRET-based assay described above for the study of the inhibition activity of **1**. The obtained results (Figures 3 and S2; Table S1) indicate that all conjugates inhibit processing of pre-miR-21 in the low micromolar range with compounds **1**, **6a**′, **6b**, **6c**, and **6c**′ being the best inhibitors with IC_{50}'s values below 5 μM. Selectivity studies performed using the same assays in the presence of MCF7 lysates showed that compounds **6b** and **6c** bear the best selectivity in the tested conditions (Table S1). It must be noted that even if the affinity of **6b** and **6c** for pre-miR-21 was improved compared to that of compound **1**, the inhibition activity remained in the same range as that for **1**.

To gain a better understanding about the molecular mechanism of interaction, we performed molecular docking studies for compounds **6b** and **6c**. Docking of **6c** with pre-miR-21 was previously illustrated in Figure 2B and C, while docking of compound **6b** is illustrated in Figure 4B and C. These studies suggested that both compounds seem to interact with the same site. More specifically, **6b** could interact with residues C16−U21 and C49-A53 while **6c** with U15-A17 and A50-C51 upon formation of hydrogen bonds, $\pi-\pi$ interactions as well as electrostatic interactions. This hypothetical binding site seems to be similar to the one of compound **1** and experimental results about binding and selectivity illustrate that both histidine and lysine are favorable amino acids for the preparation of this type of ligands. Noteworthy, nucleobases **S** and **SAr** seem to be closely involved in the interaction and the spatial distribution of the three binding domains is more accurate than the one of compound **1**, as demonstrated also experimentally by K_D values. While **6b** and **6c** are the best pre-miR-21 ligands and inhibitors, in terms of both affinity and selectivity, **6c**′ bears a three-time higher K_D value than **6b** and **6c** but very similar inhibition activity. Comparison with **6c**′ shows that the latter should interact with a different binding site located close to the cleavage site of Dicer, i.e., U27 to G28 and C41 to A42 (Supporting Information Figure S3) but with a lower number of interactions, thus being a weaker binder. The interactions proposed by the model are mainly hydrogen bonds and electrostatic interactions, but further intramolecular interactions are involved, probably hindering the correct interaction with the target and causing the observed increase in the K_D value.

To complete these studies, we decided to measure the thermodynamic parameters of the complex formed with pre-miR-21 for all the synthesized compounds in comparison with **1**. Free Gibbs energies ($\Delta G°$) were first calculated from the dissociation constants ($\Delta G° = -RT \ln K_D$) and were found to be very similar (from −36.6 to −41.5 kJ/mol), with **6b** and **6c** forming the most favorable complexes (Figure 4C). To complete the thermodynamic binding profiles, enthalpic ($\Delta H°$) and entropic ($-T\Delta S°$) energy contributions were determined after the determination of $\Delta G°_T$ at several temperatures (278−308 K). The obtained values allow for a comparison of ligands binding to the target. In all cases, the formation of ligand/pre-miR-21 complexes is driven by entropy, indicating a strong desolvation effect during interaction. The $\Delta G°$ value can be divided into the $\Delta G°_{nel}$ value, which reflects the contribution of nonelectrostatic interactions to the total free energy, such as nonionic hydrophobic effects driven by entropy, and specific interactions, including H-bonds, van der Waals interactions, and π-stacking, and the pure electrostatic (polyelectrolyte) contribution, $\Delta G°_{el}$, which reflects the ionic interactions occurring between two groups of opposite charge and is highly dependent on the salt concentration. We found that the interactions mainly involve nonelectrostatic interactions because the $\Delta G°_{nel}$ component represents 87−99% of the overall free energy (Table S2). Although this is an important

https://doi.org/10.1021/acsmedchemlett.0c00682
ACS Med. Chem. Lett. 2021, 12, 899−906

parameter that should contribute to the observed selectivity, binding could be probably improved by noncovalent interactions such as H-bonds, π-stacking, and π-ions for an increase in the enthalpy component.

In this work, we took advantage of an original binder that proved to inhibit miR-21 biogenesis in cancer cells to perform the design of a new series of pre-miR-21 ligands, based on the potential configuration of the binder/RNA complex as proposed by initial docking. These ligands were synthesized upon conjugation of three RNA binding domains, and the in vitro study of their affinity, selectivity, and inhibition activity allowed for the identification of two compounds, **6b** and **6c**, that are strong and selective binders. The study of their binding to pre-miR-21 confirmed that the three binding domains, i.e., artificial nucleobase **S**, neomycin, and histidine or lysine, act cooperatively since each separate moiety is not able to bind the target. Docking studies suggested that the binding site is located in the stem part of pre-miR-21 where two bulges induce the distortion of the double helix. Altogether, these results support the idea that the inhibition efficacy of an RNA binder depends upon both the affinity and the binding site on each pre-miRNA. Future works will be devoted to the optimization of these compounds and reducing the size of the aminoglycoside moiety with the aim to increase selectivity and enthalpic contribution to binding and to confirm their activity in cell-based studies.

■ ASSOCIATED CONTENT

Supporting Information

The Supporting Information is available free of charge at https://pubs.acs.org/doi/10.1021/acsmedchemlett.0c00682.

Binding curves and inhibition curves of compounds **1** and **6a/a′−6c/c′**; docking of the new conjugate containing neomycin, histidine, and nucleobase SAr (**6c'**) with the pre-miR-21 hairpin loop; salt effect for compounds **1** and **6a/a'−6c/c'**; IC_{50} values for the inhibition of pre-miR-21 cleavage; thermodynamic parameters for ligand−pre-miR-21 interactions; dissociation constants for pre-miR-372 binding; liquid-phase synthetic pathway for the preparation of new conjugates **6b−6c/c′**; solid-phase synthetic pathway for the preparation of uracil-containing conjugate **15** containing neomycin, nucleobase uracil, and amino acid alanine; experimental procedures; NMR spectra of reported compounds (PDF)

■ AUTHOR INFORMATION

Corresponding Author

Maria Duca − *Université Côte d'Azur, CNRS, Institute of Chemistry of Nice (ICN), 06100 Nice, France;* orcid.org/0000-0002-2666-6180; Email: maria.duca@univ-cotedazur.fr

Authors

Chloé Maucort − *Université Côte d'Azur, CNRS, Institute of Chemistry of Nice (ICN), 06100 Nice, France*

Duc Duy Vo − *Université Côte d'Azur, CNRS, Institute of Chemistry of Nice (ICN), 06100 Nice, France*

Samy Aouad − *Université Côte d'Azur, CNRS, Institute of Chemistry of Nice (ICN), 06100 Nice, France*

Coralie Charrat − *Université Côte d'Azur, CNRS, Institute of Chemistry of Nice (ICN), 06100 Nice, France*

Stéphane Azoulay − *Université Côte d'Azur, CNRS, Institute of Chemistry of Nice (ICN), 06100 Nice, France*

Audrey Di Giorgio − *Université Côte d'Azur, CNRS, Institute of Chemistry of Nice (ICN), 06100 Nice, France*

Complete contact information is available at: https://pubs.acs.org/10.1021/acsmedchemlett.0c00682

Notes

The authors declare no competing financial interest.

■ ACKNOWLEDGMENTS

Thanks are due to Institut de Recherche Servier for fellowship to C.M., to Agence Nationale de la Recherche for support and fellowship to D.D.V. (ANRJS07-011-1,) and to IDEX-JEDI of Université Côte d'Azur for fellowship to S.A.

■ REFERENCES

(1) Warner, K. D.; Hajdin, C. E.; Weeks, K. M. Principles for targeting RNA with drug-like small molecules. *Nat. Rev. Drug Discovery* **2018**, *17*, 547−58.

(2) Falese, J. P.; Donlic, A.; Hargrove, A. E. Targeting RNA with small molecules: from fundamental principles towards the clinic. *Chem. Soc. Rev.* **2021**, *50*, 2224−43.

(3) Hammond, S. M. An overview of microRNAs. *Adv. Drug Delivery Rev.* **2015**, *87*, 3−14.

(4) Ambros, V. The evolution of our thinking about microRNAs. *Nat. Med.* **2008**, *14*, 1036−40.

(5) Kim, V. N.; Han, J.; Siomi, M. C. Biogenesis of small RNAs in animals. *Nat. Rev. Mol. Cell Biol.* **2009**, *10*, 126−39.

(6) Peng, Y.; Croce, C. M. The role of MicroRNAs in human cancer. *Signal Transduct. Target. Ther.* **2016**, *1*, 15004.

(7) Li, Z.; Rana, T. M. Therapeutic targeting of microRNAs: current status and future challenges. *Nat. Rev. Drug Discovery* **2014**, *13*, 622−38.

(8) Di Giorgio, A.; Duca, M. Synthetic small-molecule RNA ligands: future prospects as therapeutic agents. *MedChemComm* **2019**, *10*, 1242−55.

(9) Disney, M. D.; Angelbello, A. J. Rational Design of Small Molecules Targeting Oncogenic Noncoding RNAs from Sequence. *Acc. Chem. Res.* **2016**, *49*, 2698−704.

(10) Pomplun, S.; Gates, Z. P.; Zhang, G.; Quartararo, A. J.; Pentelute, B. L. Discovery of Nucleic Acid Binding Molecules from Combinatorial Biohybrid Nucleobase Peptide Libraries. *J. Am. Chem. Soc.* **2020**, *142*, 19642−51.

(11) Velagapudi, S. P.; Cameron, M. D.; Haga, C. L.; Rosenberg, L. H.; Lafitte, M.; Duckett, D. R.; Phinney, D. G.; Disney, M. D. Design of a small molecule against an oncogenic noncoding RNA. *Proc. Natl. Acad. Sci. U. S. A.* **2016**, *113*, 5898−903.

(12) Velagapudi, S. P.; Gallo, S. M.; Disney, M. D. Sequence-based design of bioactive small molecules that target precursor microRNAs. *Nat. Chem. Biol.* **2014**, *10*, 291−7.

(13) Sun, L. Z.; Jiang, Y.; Zhou, Y.; Chen, S. J. RLDOCK: A New Method for Predicting RNA-Ligand Interactions. *J. Chem. Theory Comput.* **2020**, *16*, 7173−83.

(14) Ehrhardt, J. E.; Weeks, K. M. Time-Resolved, Single-Molecule, Correlated Chemical Probing of RNA. *J. Am. Chem. Soc.* **2020**, *142*, 18735−40.

(15) Kelly, M. L.; Chu, C. C.; Shi, H.; Ganser, L. R.; Bogerd, H. P.; Huynh, K.; Hou, Y.; Cullen, B. R.; Al-Hashimi, H. M. Understanding the characteristics of nonspecific binding of drug-like compounds to canonical stem-loop RNAs and their implications for functional cellular assays. *RNA* **2021**, *27*, 12−26.

(16) Paul, R.; Dutta, D.; Paul, R.; Dash, J. Target-Directed Azide-Alkyne Cycloaddition for Assembling HIV-1 TAR RNA Binding Ligands. *Angew. Chem., Int. Ed.* **2020**, *59*, 12407−11.

(17) Vo, D. D.; Becquart, C.; Tran, T. P. A.; Di Giorgio, A.; Darfeuille, F.; Staedel, C.; Duca, M. Building of neomycin-nucleobase-

amino acid conjugates for the inhibition of oncogenic miRNAs biogenesis. *Org. Biomol. Chem.* **2018**, *16*, 6262−74.
(18) Vo, D. D.; Staedel, C.; Zehnacker, L.; Benhida, R.; Darfeuille, F.; Duca, M. Targeting the production of oncogenic microRNAs with multimodal synthetic small molecules. *ACS Chem. Biol.* **2014**, *9*, 711−21.
(19) Vo, D. D.; Tran, T. P.; Staedel, C.; Benhida, R.; Darfeuille, F.; Di Giorgio, A.; Duca, M. Oncogenic MicroRNAs Biogenesis as a Drug Target: Structure-Activity Relationship Studies on New Aminoglycoside Conjugates. *Chem. - Eur. J.* **2016**, *22*, 5350−62.
(20) Cho, W. J.; Shin, J. M.; Kim, J. S.; Lee, M. R.; Hong, K. S.; Lee, J. H.; Koo, K. H.; Park, J. W.; Kim, K. S. miR-372 regulates cell cycle and apoptosis of ags human gastric cancer cell line through direct regulation of LATS2. *Mol. Cells* **2009**, *28*, 521−7.
(21) Wilson, D. N. Ribosome-targeting antibiotics and mechanisms of bacterial resistance. *Nat. Rev. Microbiol.* **2014**, *12*, 35−48.
(22) Hobson, C.; Chan, A. N.; Wright, G. D. The Antibiotic Resistome: A Guide for the Discovery of Natural Products as Antimicrobial Agents. *Chem. Rev.* **2021**, *121*, 3464−94.
(23) Thomas, J. R.; Hergenrother, P. J. Targeting RNA with small molecules. *Chem. Rev.* **2008**, *108*, 1171−224.
(24) Malnuit, V.; Duca, M.; Benhida, R. Targeting DNA base pair mismatch with artificial nucleobases. Advances and perspectives in triple helix strategy. *Org. Biomol. Chem.* **2011**, *9*, 326−36.
(25) Guianvarc'h, D.; Benhida, R.; Fourrey, J. L.; Maurisse, R.; Sun, J. S. Incorporation of a novel nucleobase allows stable oligonucleotide-directed triple helix formation at the target sequence containing a purine.pyrimidine interruption. *Chem. Commun.* **2001**, 1814−5.
(26) Medina, P. P.; Nolde, M.; Slack, F. J. OncomiR addiction in an in vivo model of microRNA-21-induced pre-B-cell lymphoma. *Nature* **2010**, *467*, 86−90.
(27) Costales, M. G.; Aikawa, H.; Li, Y.; Childs-Disney, J. L.; Abegg, D.; Hoch, D. G.; Pradeep Velagapudi, S.; Nakai, Y.; Khan, T.; Wang, K. W.; Yildirim, I.; Adibekian, A.; Wang, E. T.; Disney, M. D. Small-molecule targeted recruitment of a nuclease to cleave an oncogenic RNA in a mouse model of metastatic cancer. *Proc. Natl. Acad. Sci. U. S. A.* **2020**, *117*, 2406−11.
(28) Garner, A. L.; Lorenz, D. A.; Sandoval, J.; Gallagher, E. E.; Kerk, S. A.; Kaur, T.; Menon, A. Tetracyclines as Inhibitors of Pre-microRNA Maturation: A Disconnection between RNA Binding and Inhibition. *ACS Med. Chem. Lett.* **2019**, *10*, 816−21.
(29) Lorenz, D. A.; Vander Roest, S.; Larsen, M. J.; Garner, A. L. Development and Implementation of an HTS-Compatible Assay for the Discovery of Selective Small-Molecule Ligands for Pre-microRNAs. *SLAS Discov* **2018**, *23*, 47−54.
(30) Naro, Y.; Ankenbruck, N.; Thomas, M.; Tivon, Y.; Connelly, C. M.; Gardner, L.; Deiters, A. Small Molecule Inhibition of MicroRNA miR-21 Rescues Chemosensitivity of Renal-Cell Carcinoma to Topotecan. *J. Med. Chem.* **2018**, *61*, 5900−09.
(31) Suresh, B. M.; Li, W.; Zhang, P.; Wang, K. W.; Yildirim, I.; Parker, C. G.; Disney, M. D. A general fragment-based approach to identify and optimize bioactive ligands targeting RNA. *Proc. Natl. Acad. Sci. U. S. A.* **2020**, *117*, 33197−203.
(32) Llano-Sotelo, B.; Azucena, E. F., Jr.; Kotra, L. P.; Mobashery, S.; Chow, C. S. Aminoglycosides modified by resistance enzymes display diminished binding to the bacterial ribosomal aminoacyl-tRNA site. *Chem. Biol.* **2002**, *9*, 455−63.
(33) Detering, C.; Varani, G. Validation of automated docking programs for docking and database screening against RNA drug targets. *J. Med. Chem.* **2004**, *47*, 4188−201.
(34) Shi, Z.; Zhang, J.; Qian, X.; Han, L.; Zhang, K.; Chen, L.; Liu, J.; Ren, Y.; Yang, M.; Zhang, A.; Pu, P.; Kang, C. AC1MMYR2, an inhibitor of dicer-mediated biogenesis of Oncomir miR-21, reverses epithelial-mesenchymal transition and suppresses tumor growth and progression. *Cancer Res.* **2013**, *73*, 5519−31.
(35) Baisden, J. T.; Boyer, J. A.; Zhao, B.; Hammond, S. M.; Zhang, Q. Visualizing a protonated RNA state that modulates microRNA-21 maturation. *Nat. Chem. Biol.* **2021**, *17*, 80−8.
(36) Lau, P. W.; Guiley, K. Z.; De, N.; Potter, C. S.; Carragher, B.; MacRae, I. J. The molecular architecture of human Dicer. *Nat. Struct. Mol. Biol.* **2012**, *19*, 436−40.
(37) Tran, T. P.; Vo, D. D.; Di Giorgio, A.; Duca, M. Ribosome-targeting antibiotics as inhibitors of oncogenic microRNAs biogenesis: Old scaffolds for new perspectives in RNA targeting. *Bioorg. Med. Chem.* **2015**, *23*, 5334−44.
(38) Aradi, K.; Di Giorgio, A.; Duca, M. Recent progresses in aminoglycoside conjugation for RNA targeting: antimicrobials and beyond. *Chem. - Eur. J.* **2020**, *26*, 12273−309.
(39) Bera, S.; Mondal, D.; Palit, S.; Schweizer, F. Structural modifications of the neomycin class of aminoglycosides. *MedChemComm* **2016**, *7*, 1499−534.
(40) Thamban Chandrika, N.; Garneau-Tsodikova, S. Comprehensive review of chemical strategies for the preparation of new aminoglycosides and their biological activities. *Chem. Soc. Rev.* **2018**, *47*, 1189−249.

https://doi.org/10.1021/acsmedchemlett.0c00682
ACS Med. Chem. Lett. 2021, 12, 899−906